encit 2020

ABCM
Associação Brasileira de Engenharia e Ciências Mecânicas

18th Brazilian Congress of Thermal Sciences and Engineering
November 16-20, 2020 (Online)

ENCIT2020-0172
Reconstruction of spatio-temporal flow datasets via kernel-based non-linear proper orthogonal decomposition

Rebeca P Marcondes
Tulio R. Ricciardi
William R. Wolf
School of Mechanical Engineering, Universidade Estadual de Campinas, Campinas, SP 13083-860, Brasil
rebecapereiramarc@hotmail.com
tulioricci@gmail.com
wolf@fem.unicamp.br

Abstract. *Proper orthogonal decomposition, POD, has been widely used in the community of fluid dynamics. The POD finds application in analysis of coherent flow structures, data compression and construction of reduced-order models, ROMs. However, in the latter case, ROMs are typically unstable for problems that present strong non-linearities, such as shock waves and contact surfaces, or a broad range of temporal and spatial scales, in turbulent flows. The kernel proper orthogonal decomposition KPOD is a promising method for overcoming the previous issues since it maps the non-linear data into a higher dimension, known as feature space, using kernel functions. One expects that non-linear features are incorporated in the KPOD basis such that fewer modes are required for a better approximation of the data. In this work, we employ both the POD and KPOD for the reconstruction of non-linear solutions from a modified Shu-Osher shock tube problem and the Ginzburg-Landau equation. A Radial Basis Function Neural Network is applied for the reconstructions and results show that the KPOD is a promising technique compared to the standard POD.*

Keywords: *Proper orthogonal decomposition (POD), principal component analysis (PCA), kernel methods, dataset reconstruction, neural networks*

1. INTRODUCTION

Proper Orthogonal Decomposition, POD, was first applied in the fluid dynamics field by (Lumley, 1967) to extract coherent structures from turbulent flows. Since then, POD has become a tool of paramount importance for other applications in the field, such as reduced-order modeling based on projection techniques (Aubry *et al.*, 1989). Recently, Ribeiro and Wolf (2017) employed several variations of POD for the investigation of coherent structures in the turbulent flow past an airfoil at moderate Reynolds number. The application of POD in the context of reduced-order modeling brings challenges when problems carry strong non-linearities. In this case, since POD is a linear decomposition, a large number of POD modes is required to reconstruct a flow field, what usually leads to numerical instabilities. Turbulent flows and compressible flows involving shock waves suffer from this problem sine they involve a large disparity in spatial and temporal scales.

Alternative non-linear decomposition methods, such as Kernel Proper Orthogonal Decomposition, KPOD, also referred to in the literature as Kernel Principal Component Analysis, KPCA, (Scholkopf *et al.*, 1999) may shed light into this problem. The KPOD technique projects input data into a feature space with a higher dimension and then performs standard proper orthogonal decomposition of that new space. It has been applied successfully in several applications such as image denoising (Mika *et al.*, 1999) and novelty detection (Hoffmann, 2007), where the authors find abnormal data into the training dataset. The method has also been applied for control of nonlinear processes (Zhou *et al.*, 2019) and for spatial-temporal analysis of the events occurring on planet Earth (Bueso *et al.*, 2020).

However, to our knowledge, the current method has not been applied specifically in the fluid dynamics field. In this work, we provide a fist comparison between POD and KPOD for reconstruction of spatio-temporal datasets obtained by the solution of partial differential equations that model fluid dynamics processes. We first apply the method for problems involving discontinuities in their solution. In this case, we solve a modified Shu-Osher shock tube problem with strong discontinuities and shock-shock interaction. Then, we solve a model problem that allows a chaotic solution mimicking a turbulent field. In this case, the complex Ginzburg-Landau equation is solved. While reconstruction of the fluctuation field is straightforward with POD, the same cannot be said for KPOD. Since the latter method is applied in a higher

dimensional feature space, the fluctuation field reconstruction needs to be performed in the original feature space. Here, we present a technique that allows this reconstruction using neural networks. We compare results obtained by the POD and KPOD reconstructions in a fair way, using the same methodology that consists of a Radial Basis Function Neural Network, RBF-NN.

2. THEORETICAL AND NUMERICAL FORMULATION

2.1 Proper Orthogonal Decomposition

In fluid mechanics, Proper Orthogonal Decomposition, POD, also known as Principal Component Analysis, PCA, in statistics, is based on the factorization of a spatial-temporal data matrix obtained from simulations or experiments. The method is based on singular value decomposition, SVD, and attempts to find a linear subspace of lower dimensional than the original data. Through SVD, it is possible to computed POD modes which are ranked in an energetic sense according to its residual variance (Lumley, 1967).

The goal of POD is to project a zero mean dataset $\mathbf{X} = [\mathbf{x_1}, \mathbf{x_2}, \ldots, \mathbf{x_N}] \in \mathbb{R}^{M\times N}$ into a sub-space $\mathbb{R}^{D\times N}$, where $D \ll N \ll M$. In general, for numerical simulations, we have M and N representing the number of spatial and temporal elements in the dataset. The projection can be obtained directly by the SVD or it can be computed using a covariance matrix $\mathbf{C} \in \mathbb{R}^{M\times M}$ as

$$\mathbf{C} = \frac{1}{N}\sum_{j=1}^{N} \mathbf{x_j}\mathbf{x_j}^T \,, \tag{1}$$

where $\mathbf{C}$ is a symmetric positive definite matrix. In general, for numerical simulations that generate big data problems, the snapshot POD method (Sirovich, 1987) is more indicated since it builds the covariance matrix with the transpose $\mathbf{X}$ data matrix. This leads to a covariance matrix $\mathbf{C} \in \mathbb{R}^{N\times N}$ which has a reduced size since $N \ll M$, but with the same eigenvalues and eigenvectors. Hence, the basis vectors are found by the eigen-decomposition problem

$$\mathbf{C}\alpha = \lambda\alpha \,. \tag{2}$$

where the eigenvalues λ are always positive and the eigenvectors, or temporal modes, $\alpha \in \mathbb{R}^{D\times M}$ are orthonormal amongst themselves.

A second orthogonal base can be obtained by projecting the eigenvectors α in the original dataset, leading to a sub-space $\mathbb{R}^{M\times D}$. These two orthogonal bases are sufficient to approximate the original data set with minimal loss of information in a L2 norm sense.

2.2 Kernel Proper Orthogonal Decomposition

The Kernel Proper Orthogonal Decomposition, KPOD, also known in literature as Kernel Principal Component Analysis, KPCA, (Scholkopf *et al.*, 1999) is an nonlinear form of the Proper Orthogonal Decomposition that uses kernel techniques to map the input data into a high dimensional feature space $x_i \rightarrow \Phi(x_i)$. Similarly to POD, the KPOD method requires the data to be centered ($\sum_{k=1}^{M}\hat{\Phi}(x_k) = \sum_{k=1}^{M}\left(\Phi(x) - \overline{\Phi}\right) = 0$), where $\overline{\Phi} = \frac{1}{M}\sum_{j=1}^{M}\Phi(x_j)$. Following the ideas of linear POD, we can solve an eigenvalue problem building a covariance matrix in the feature space expressed as

$$\overline{\mathbf{C}} = \frac{1}{M}\sum_{j=1}^{M} \hat{\Phi}(x_j)\hat{\Phi}(x_j)^T \,, \tag{3}$$

what leads to the following eigenvalue problem in the higher dimensional space

$$\lambda\mathbf{V} = \overline{\mathbf{C}}\mathbf{V} \,. \tag{4}$$

To solve this decomposition problem, the following equation must be considered

$$\lambda(\hat{\Phi}(x_k)\cdot\mathbf{V}) = (\hat{\Phi}(x_k)\cdot\overline{\mathbf{C}}\mathbf{V}) \,, \tag{5}$$

where the eigenvector $\mathbf{V}$ is given by a linear combination of $[\hat{\Phi}(x_1), \hat{\Phi}(x_2), ..., \hat{\Phi}(x_M)]$

$$\mathbf{V} = \sum_{i=1}^{M} \alpha_i\hat{\Phi}(x_i) \,. \tag{6}$$

In order to avoid working explicitly with $\Phi(x)$, we work with kernel functions that can be described by

$$\overline{k}(x,y) = \hat{\Phi}(x)^T \hat{\Phi}(y) = (\Phi(x) - \overline{\Phi})^T (\Phi(y) - \overline{\Phi}) \, . \tag{7}$$

This procedure is called the kernel trick and it is an explicit form of nonlinear mapping of Eq. (3). Therefore, in the feature space a kernel function can be chosen directly to represent the dot product $K_{ij} = (\Phi(x_i) \cdot \Phi(x_j))$. To compute the centered kernel matrix $\overline{\mathbf{K}}$ from $\mathbf{K}$ directly, one can use the following equation

$$\overline{k}(x,y) = k(x,y) - \frac{1}{M}\sum_{j=1}^{M} k(x,y_j) - \frac{1}{M}\sum_{i=1}^{M} k(x_i,y) + \frac{1}{M^2}\sum_{i=1}^{M}\sum_{j=1}^{M} k(x_i,y_j) \, , \tag{8}$$

which can be described in short notation as

$$\overline{\mathbf{K}} = \mathbf{K} - \frac{1}{M}\mathbf{K}\,\mathbf{1}\mathbf{1}^T - \frac{1}{M}\,\mathbf{1}\mathbf{1}^T\mathbf{K} + \frac{\mathbf{1}^T\mathbf{K}\,\mathbf{1}}{M^2}\,\mathbf{1}\mathbf{1}^T \, . \tag{9}$$

In the previous equation, the term $\mathbf{1} \in \mathbb{R}^{N\times 1}$ and, hence, is a vector of unitary elements. The second, third and fourth terms of Eq. (9) represent the sum of columns, rows and all elements in the kernel matrix of Eq. (8), respectively.

Substituting Eqs. (3) and (6) into Eq. (5), the eigenvalue problem becomes

$$l\lambda\alpha = \mathbf{K}\alpha \, . \tag{10}$$

Once the solution of Eq. (10) is determined, the outputs must be normalized so that the corresponding vector in the feature space is also normalized

$$\sum_{i,j=1}^{l} \alpha_i^k \alpha_j^k (\Phi(x_i) \cdot \Phi(x_j)) = (\alpha^k \cdot \mathbf{K}\,\alpha^k) = \lambda_k(\alpha^k \cdot \alpha^k) = 1 \, . \tag{11}$$

Finally, for principal component extraction, projections of $\Phi(x_i)$ onto the eigenvectors $\mathbf{V}$ into the feature space can be computed as

$$(V^k \cdot \Phi(x)) = \sum_{i=1}^{l} \alpha_i^k (\Phi(x_i) \cdot \Phi(x)) = \sum_{i=1}^{l} \alpha_i^k K(x_i,x) \, . \tag{12}$$

Different kernel functions can be employed in the KPOD method and represent a hyperparameter of the approach. In the present work, the following polynomial

$$k(x,y) = [\gamma(x^T y) + c]^d \, , \tag{13}$$

and radial basis function kernels are applied

$$k(x,y) = \exp\big(-\gamma||x-y||^2\big). \tag{14}$$

In the above equations, the term d sets the polynomial degree, c is an independent coefficient and γ is the kernel width. These terms are also hyperparameters of the KPOD technique and should be chosen according to the specific problem at hand.

3. DATA RECONSTRUCTION VIA NEURAL NETWORKS

Flow modal decomposition techniques provide bases functions that can be used for several applications ranging from detection of coherent patterns, construction of reduced-order models and flow reconstruction with data compression. In the linear POD, reconstruction is a linear problem and requires the product of temporal modes and spatial eigenfunctions. However, since the KPOD method consists in the projection of the input data to another dimension, the reconstruction problem results into a non-linear optimization problem which can be tricky.

Reconstruction via KPOD can be solved by numerous methods, for example kernel ridge regression. However, this approach produces a dataset with the same dimensions of the original data. In this work, we choose to use the Radial Basis Function Neural Network, RBF-NN, (Broomhead and Lowe, 1988) due to its simplicity and dataset compression capability. More complex neural networks could be used but the present one provides a good cost-benefit since its usual form has only one hidden layer with two hyperparameters: the standard deviation and the number of clusters.

The input to the RBF-NN consists on the eigenvalues multiplied by the eigenvectors which result from the decomposition. The reconstruction is then given by

$$\mathbf{y} = \sum_{i=1}^{n} w_i k(\mathbf{x}, \mathbf{c_i}), \tag{15}$$

where n is the number of neurons in the hidden layers, k is the activation function of each neuron given by Eq. (14), $\mathbf{c_i}$ is the center vector for each RBF function, calculated by the K-means method (MacQueen, 1967) and $\mathbf{w_i}$ is the weight of neuron i in the output neuron. The standard deviation is calculated by:

$$\sigma = \frac{d_{max}}{\sqrt{2r}}, \tag{16}$$

where d_{max} is the maximum distance between any two cluster centers and r is the number of clusters. In order to have fair comparisons between the POD and KPOD flow reconstructions, the RBF-NN is used with both approaches. It is important to mention that the neural networks have improved the POD reconstructions compared to the usual procedure.

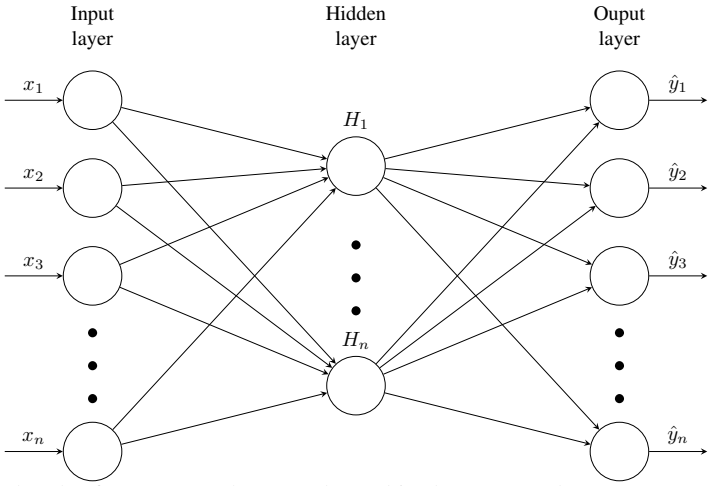

Figure 1: Sketch of RBF Neural Network used in the POD and KPOD reconstructions.

4. RESULTS

This section presents results of application of KPOD in the reconstruction of non-linear solutions from partial difference equations. A shock tube problem is first presented followed by the solution of the complex Ginzburg-Landau equation.

4.1 Solution of modified Shu-Osher shock tube problem

Shock tubes are important devices used in the field of gas dynamics to study shock waves. The unsteady flow-field developing along the tube contains strong non-linearities given by a shock wave and a contact surface that propagate along the driven gas section (low pressure region), while an expansion wave propagates into the driver gas section. In the present case, the solutions of the shock tube problem are obtained by solving the one-dimensional Euler equations as

$$\begin{aligned} &\frac{\partial \rho}{\partial t} + \frac{\partial \rho u}{\partial x} = 0\,, \\ &\frac{\partial \rho u}{\partial t} + \frac{\partial \rho u^2 + p}{\partial x} = 0\,, \\ &\frac{\partial E}{\partial t} + \frac{\partial (p+E)u}{\partial x} = 0\,. \end{aligned} \tag{17}$$

In the above equations, ρ, u, p and E represent the density, velocity, pressure and total energy per unit volume, respectively. This set of equations is closed by the ideal gas equation.

Since the shock tube problem allows discontinuities in the solution, it is an excellent candidate for testing the flow reconstruction capabilities of the POD. The shock waves appearing in the flow should require a large number of POD modes to avoid oscillations arising from the Gibbs phenomenon. In order to add more complexity to the solution, a modified Shu-Osher (Shu and Osher, 1989) shock tube is solved as suggested by Ramos and Wolf (2016). Here, we start the flow with two strong discontinuities that move towards the center of the tube. Density fluctuations with low

wave-numbers are imposed on the low pressure region and their interaction with the shock waves should produce higher wave-number waves, simulating shock-turbulence interaction.

We present results in terms of pressure field reconstruction in Figs. 2, 3 and 4. These figures present results for the full order model (FOM), the linear POD and the non-linear KPOD. The FOM solution is obtained by a high-order compact finite difference scheme with a localized artificial dissipation method for shock capturing (details can be found in Ramos and Wolf (2016)). The POD and KPOD reconstructions are performed using 5, 25 and 50 modes for different instants of the flow.

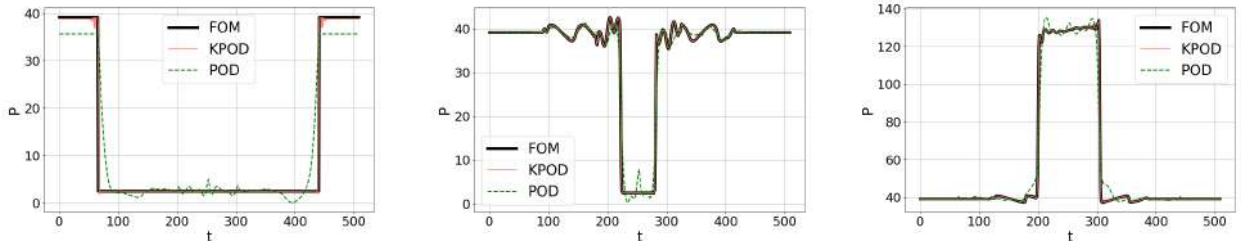

(a) Initial solution (b) Solution before shock-shock interaction (c) Solution after shock-shock interaction

Figure 2: Reconstruction with 5 modes

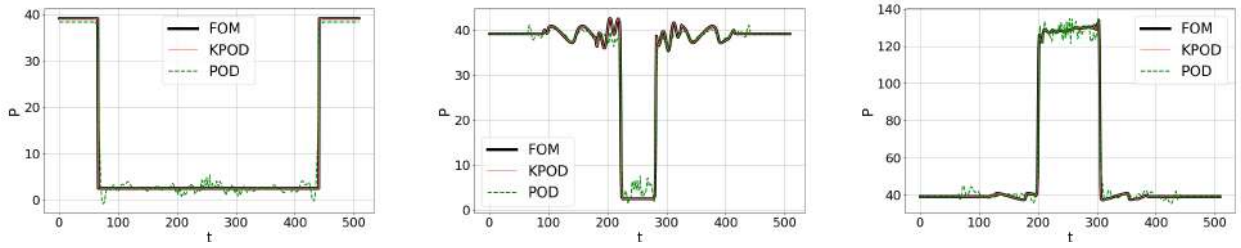

(a) Initial solution (b) Solution before shock-shock interaction (c) Solution after shock-shock interaction

Figure 3: Reconstruction with 25 modes

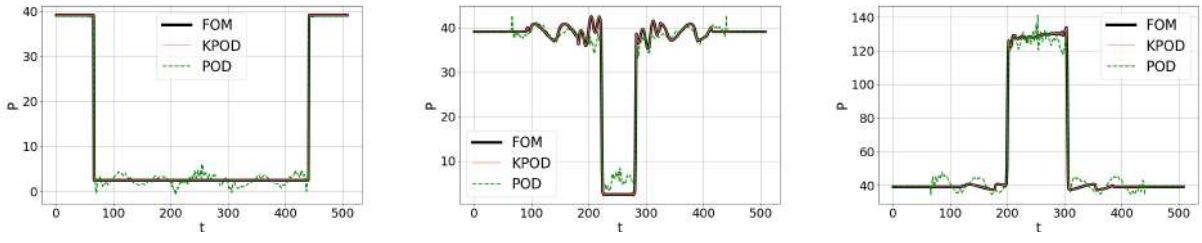

(a) Initial solution (b) Solution before shock-shock interaction (c) Solution after shock-shock interaction

Figure 4: Reconstruction with 50 modes

The initial solution depicted in the figures shows two strong initial shocks where the pressure ratio is almost 40. One can see that the flow reconstruction with POD (referred to as PCA in the figures) cannot represent the sharp pressure variations. When 5 POD modes are used, a mismatch in the high pressure levels are observed and a diffuse shock can be perceived. When more modes are employed, the high pressure levels and discontinuities are recovered but the low pressure plateau still presents high frequency oscillations from the higher POD modes. It is clear that KPOD can represent the non-linearities of the solution in a better way than the POD. The solution obtained with 5 modes has only few oscillations on the shock while reconstructions with 25 and 50 modes show a perfect agreement with the FOM solution.

Solutions obtained before and after the shock waves interact are also shown. One can also see in these solutions that physical low and high frequencies are present. These frequencies appear due to density fluctuations imposed in the initial solution. For all cases, it is possible to observe that the KPOD is able to fully reconstruct the pressure field while the POD solutions contain spurious oscillations. Increasing the number of POD modes from 5 to 50 does not seem to improve the

reconstructions while 5 KPOD modes show an excellent agreement against the FOM results. Table 1, presents the mean square error of the KPOD and POD reconstructions compared with that of the FOM. One can see that adding further modes monotonically reduces the errorof the KPOD method while in the POD case, the error is still high.

Table 1: Mean square error comparison of POD and KPOD reconstructions with the RBF neural network

	POD	KPOD
5 modes	14.74	2.87×10^{-2}
25 modes	3.49	2.88×10^{-5}
50 modes	4.37	5.88×10^{-6}

4.2 Solution of complex Ginzburg-Landau equation

The Ginzburg-Landau equations are non-linear partial differential equations that serve as models for chaotic physical systems. It allows the development of multiple spatio-temporal scales which can be representative, for example, of turbulent flows. Here, the complex Ginzburg-Landau equation is numerically solved using the technique described in Willers and Twizell (2003). The equation is given by

$$\frac{\partial A}{\partial t} = (1+i\alpha)\frac{\partial^2 A}{\partial x^2} + A - (1+i\beta)|A|^2 A\,. \tag{18}$$

Here, i is the imaginary unit and the parameters α and β are set as 2 and -2, respectively. The initial solution is set as $A = 1$ with added noise.

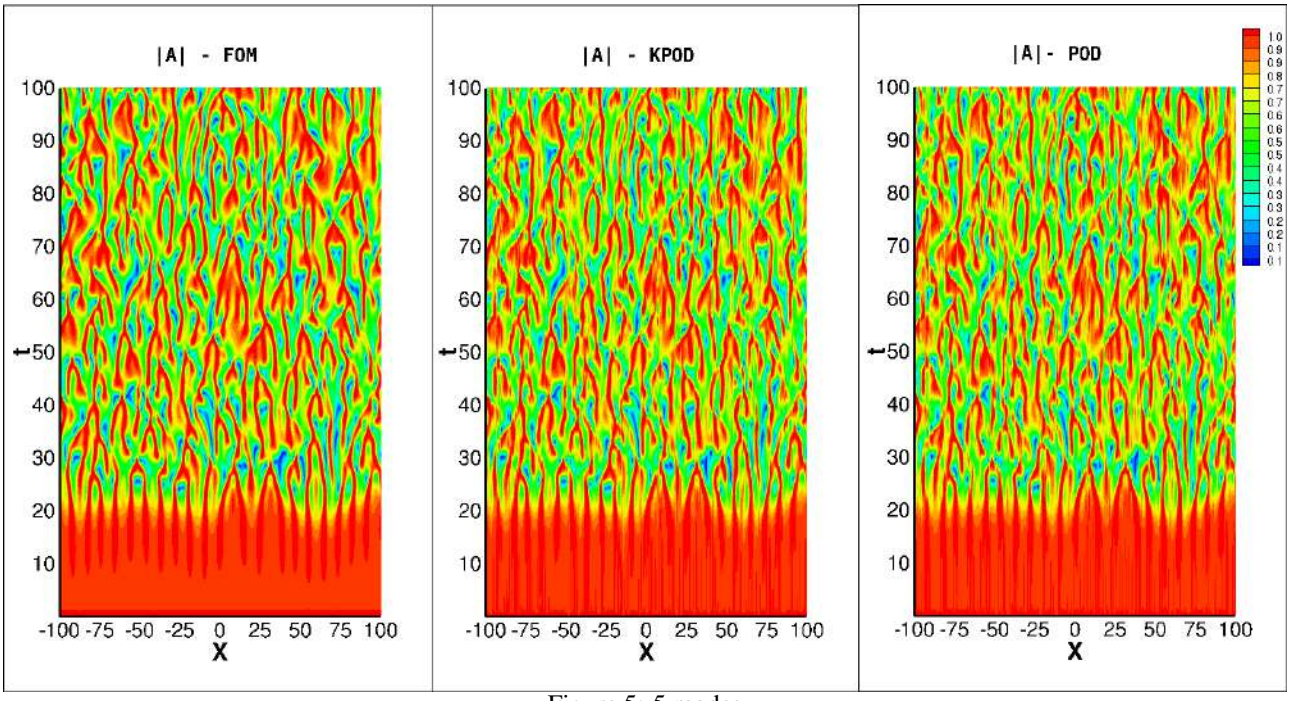

Figure 5: 5 modes

For the set of parameters and initial solution chosen, the solution becomes chaotic as can be seen in Figs. 5, 6 and 7. This figure shows the spatio-temporal development of variable A computed by the FOM. Field reconstructions are obtained by the POD and KPOD methods. Some discrepancies are observed for both methods when 5 modes are used in the reconstructions. However, the solutions show a better agreement with that of the FOM when 25 and 50 modes are employed. It is clear that visual inspection does not allow a full assessment of the error for the two methods.

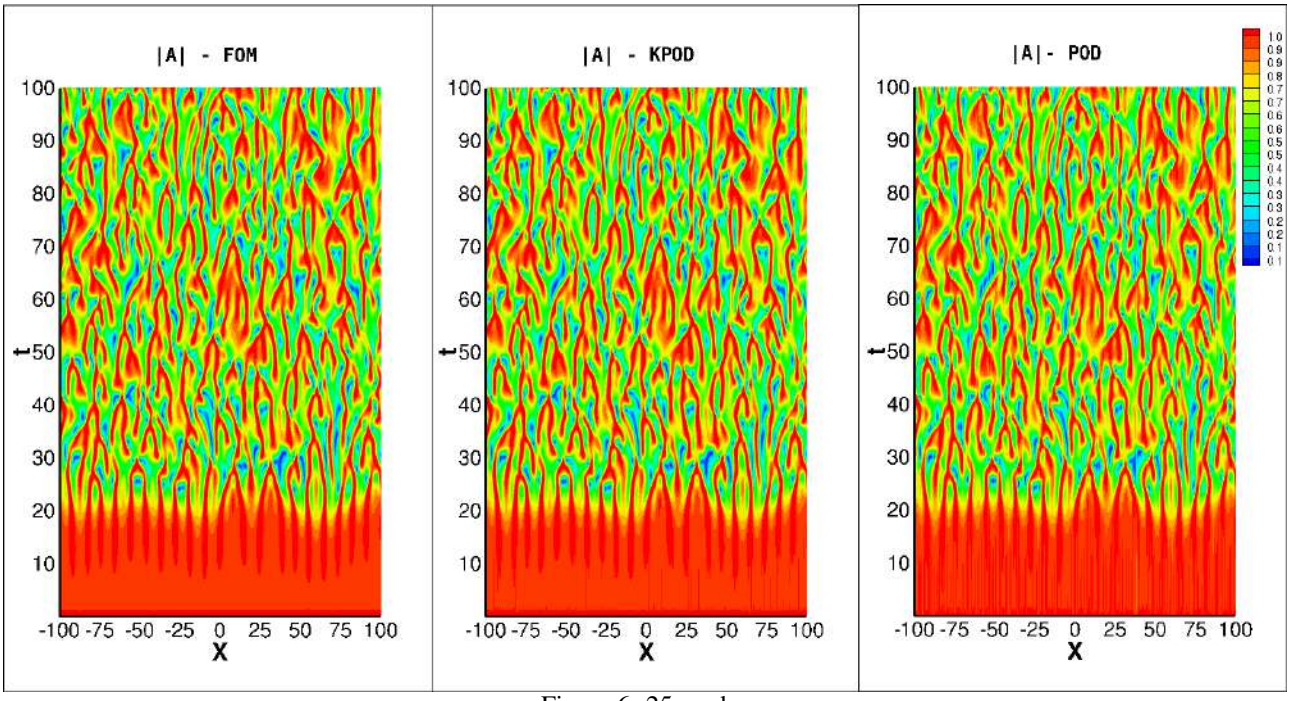

Figure 6: 25 modes

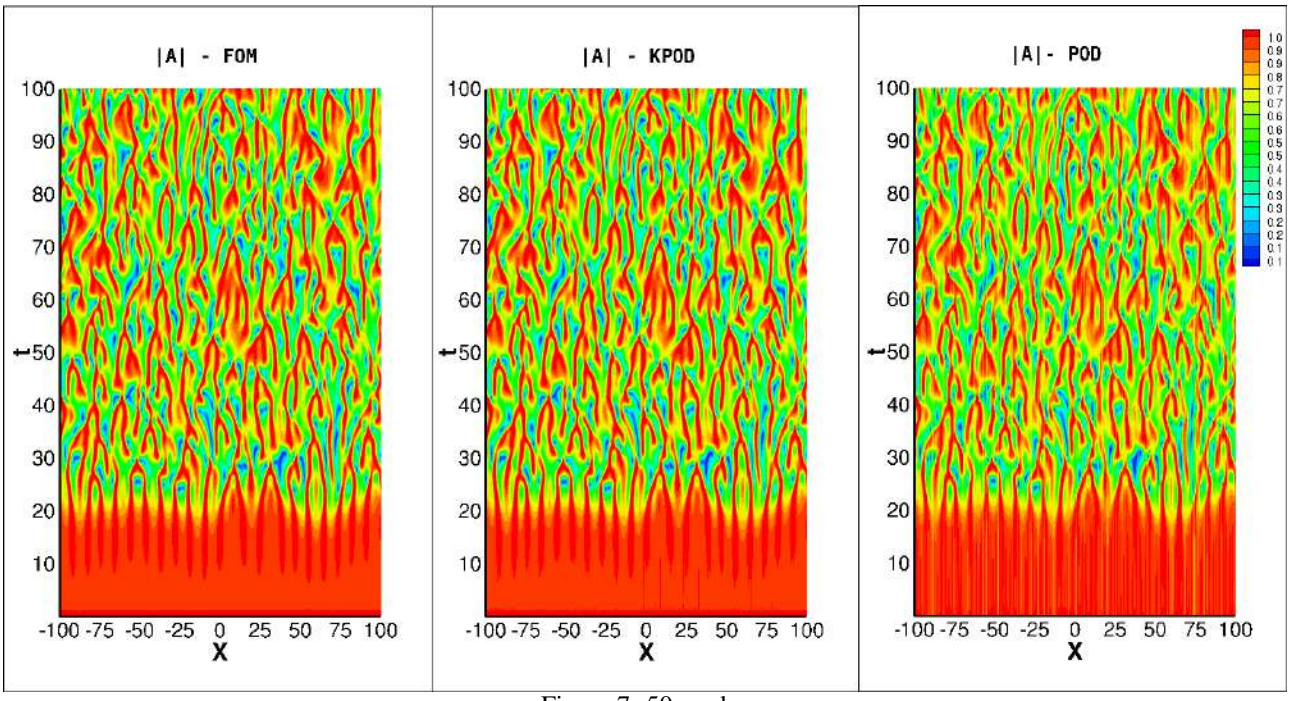

Figure 7: 50 modes

In order to have a more accurate metric, Table 2 presents the mean square error of the reconstructions for both ther POD and KPOD techniques. It is clear that adding more modes in the KPOD reconstruction leads to a convergence of the error while for the POD, the error is not further reduced.

Table 2: Mean square error of POD and KPOD reconstructions with the RBF neural network

	POD	KPOD
5 modes	5.01×10^{-3}	4.01×10^{-3}
25 modes	1.76×10^{-3}	5.57×10^{-5}
50 modes	5.31×10^{-3}	3.69×10^{-6}

5. CONCLUSIONS AND ADDITIONS TO THE FINAL PAPER

In this work, we present a comparison of modal decomposition techniques for the reconstruction of flowfield spatio-temporal datasets. Both the POD and KPOD are tested with non-linear solutions from a modified Shu-Osher shock tube problem, which serves as a model for shock-turbulence interaction. Datasets obtained from the solution of the complex Ginzburg-Landau equation are also tested. This equation allows chaotic solutions that serve as a model for turbulent flows with a broad range of spatial and temporal scales. Reconstructions are performed by a Radial Basis Function Neural Network. Results obtained by the KPOD for the shock tube can recover the original flowfield computed by a high-fidelity model while those from POD present high-frequency oscillations. Further studies are required to provide a more complete analysis of the KPOD technique and they will be shown in the final version of the paper.

6. ACKNOWLEDGEMENTS

The first author is supported by a CAPES scholarship which is acknowledged here. Authors acknowledge Fundação de Amparo à Pesquisa do Estado de São Paulo, FAPESP, for supporting the present work under research grants No. 2013/08293-7 and 2013/07375-0.

7. REFERENCES

Aubry, N., Holmes, P., Lumley, J.L. and Stone, E., 1989. "Application of dynamical system theory to coherent structures in the wall region". *Physica D: Nonlinear Phenomena*, Vol. 37, No. 1, pp. 1 – 10. ISSN 0167-2789. doi: https://doi.org/10.1016/0167-2789(89)90112-7.

Broomhead, D. and Lowe, D., 1988. "Radial basis functions, multi-variable functional interpolation and adaptive networks". *Royal Signals and Radar Establishment(United Kingdom)*, Vol. RSRE-MEMO-4148, p. 39.

Bueso, D., Piles, M. and Camps-Valls, G., 2020. "Nonlinear pca for spatio-temporal analysis of earth observation data". *IEEE Transactions on Geoscience and Remote Sensing*, pp. 1–12.

Hoffmann, H., 2007. "Kernel pca for novelty detection". *Pattern Recognition*, Vol. 40, pp. 863–874. doi: 10.1016/j.patcog.2006.07.009.

Lumley, J.L., 1967. "The structure of inhomogeneous turbulence". *Atmosphere Turbulence Radio Wave Propagation*, Vol. 790, p. 166–178.

MacQueen, J., 1967. "Some methods for classification and analysis of multivariate observations". In *Proceedings of the Fifth Berkeley Symposium on Mathematical Statistics and Probability, Volume 1: Statistics*. University of California Press, Berkeley, Calif., pp. 281–297.

Mika, S., Schölkopf, B., Smola, A., Müller, K.R., Scholz, M. and Rätsch, G., 1999. "Kernel pca and de-noising in feature spaces". In *Proceedings of the 1998 Conference on Advances in Neural Information Processing Systems II*. MIT Press, Cambridge, MA, USA, p. 536–542. ISBN 0262112450.

Ramos, B. and Wolf, W., 2016. "Aplicação de métodos numéricos de alta resolução para a solução de escoamentos compressíveis com interação choque-turbulência". doi:10.19146/pibic-2016-50673.

Ribeiro, J.H.M. and Wolf, W.R., 2017. "Identification of coherent structures in the flow past a naca0012 airfoil via proper orthogonal decomposition". *Physics of Fluids*, Vol. 29, No. 8, p. 085104. doi:10.1063/1.4997202.

Scholkopf, B., Smola, A. and Müller", K.R., 1999. "Kernel principal component analysis". In *Advances in Kernel Methods - Support Vector Learning*. MIT Press, pp. 327–352.

Shu, C.W. and Osher, S., 1989. "Efficient implementation of essentially non-oscillatory shock-capturing schemes, ii". *Journal of Computational Physics*, Vol. 83, No. 1, pp. 32 – 78. ISSN 0021-9991. doi:https://doi.org/10.1016/0021-9991(89)90222-2.

Sirovich, L., 1987. "Turbulence and the dynamics of coherent structures. iii. dynamics and scaling". *Quarterly of Applied Mathematics*, Vol. 45, pp. 583–590. doi:10.1090/qam/910464.

Willers, J. and Twizell, E., 2003. "A finite-difference solution of the ginzburg–landau equation". *Journal of Difference Equations and Applications*, Vol. 9, No. 12, pp. 1059–1068. doi:10.1080/1023619031000146896.

Zhou, Z., Du, N., Xu, J., Li, Z., Wang, P. and Zhang, J., 2019. "Randomized kernel principal component analysis for modeling and monitoring of nonlinear industrial processes with massive data". *Industrial & Engineering Chemistry Research*, Vol. 58, No. 24, pp. 10410–10417. doi:10.1021/acs.iecr.9b00300.

8. RESPONSIBILITY NOTICE

The authors are solely responsible for the printed material included in this paper.